Transmission-line models for single-layer solenoid inductors

Bart H. McGuyer

https://bartmcguyer.com/notes/note-13-CoiledLines.pdf

TL;DR: One-dimensional discrete network and continuous transmission-line toy models for close-wound solenoid inductors.

It's interesting that a solenoid inductor made from a single layer of closely wound wire can behave like a simple uniform transmission line, because of all the inductive and capacitive couplings between the turns. To explore how that works, this note derives modified Telegrapher's equations from a discrete model of a network of coupled turns and examines various approximations and properties. This was useful for some of my previous work.[1–3]
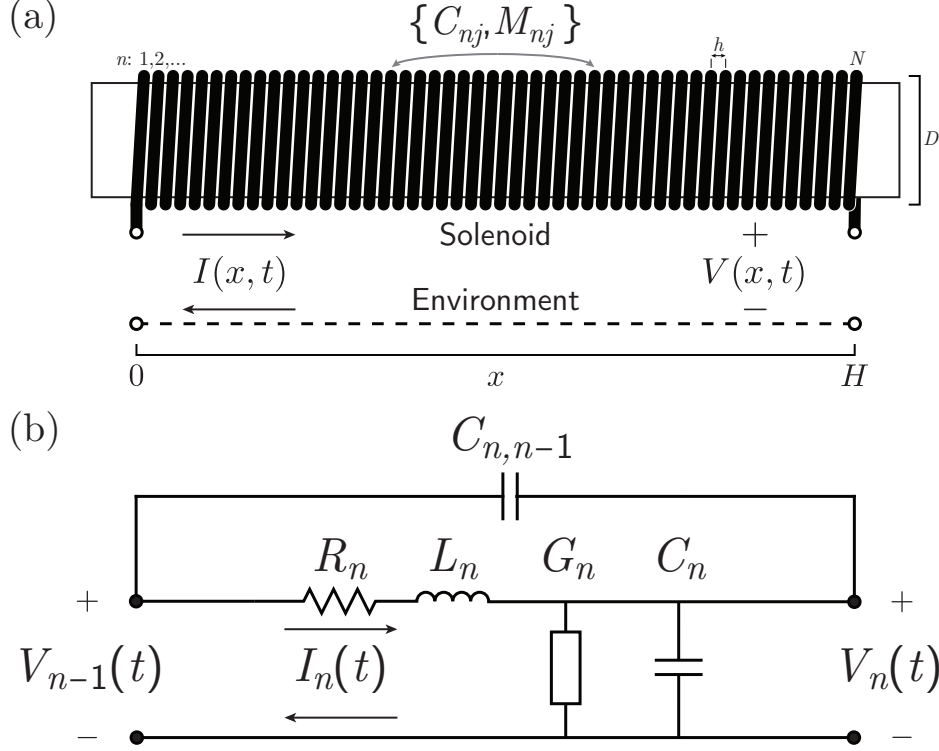
CONTENTS

FIG. 1. Setup. (a) Solenoid as a transmission line with its grounded environment as the second wire. (b) Network model unit cell for the n-th turn. Does not show inter-turn couplings except for nearest-neighbor capacitances. The unit cells for continuous transmission-line models are similar.

I. SETUP

This note's meant to complement the resources I've found on solenoids for my own reference.[a] Solenoids are very well understood, of course, but detailed treatments tend to jump straight to approximate field models like the sheath helix. Instead, the approach here provides toy models starting from a network point of view with a clear circuit interpretation. The closest works I've found are Refs. 4–8, which are mentioned below.

To begin, consider a solenoid like the one shown in Fig. 1(a). Let's assume it's made of a single layer of wire that's reasonably closely wound around a cylindrical form with an air core (non-magnetic, non-conductive). The wire by itself is a classic example of a two-wire transmission-line system, with its environment serving as the second wire. Winding the wire into the solenoid introduces new longitudinal couplings between the different segments of the wire. These couplings make such a coiled transmission line rather different than a classic straight transmission line. To examine how, let's assume that there are a large number N of turns (e.g., $N \gg 10$) and that the current and voltage vary little across each individual turn. We can then approximately model each turn with a lumped-element equivalent circuit like the unit cell shown in Fig. 1(b). Starting from a unit cell, we can setup a discrete network model and then convert it to a continuous model similar to the Telegrapher's equations for

---

[a] Also, to finally compile and complete some old notes leftover mainly from graduate school.

a transmission line.

To keep things simple, let's ignore coupling with other external circuits. For a related treatment of that topic, please see Refs. 1 and 2, which also discuss simplifying transmission-line models back to lumped-element equivalent circuits.

II. NETWORK MODEL

Consider a network of N turns indexed by $n \in [1, N]$. Let $V_n(t)$ and $I_n(t)$ be the voltage and current for the n-th turn, as sketched in Fig. 1(b). Let $n = 0$ be the input to the first turn ($n = 1$) and $n = N$ be the output after the last turn ($n = N$). By convention, each current $I_n(t)$ is positive when it flows towards higher n.

For each unit cell like the one in Fig. 1(b), the voltages and currents evolve as

$$V_n(t) - V_{n-1}(t) = -\left(R_n + L_n \frac{d}{dt}\right) I_n(t) + V_{\text{tt},n}(t) \tag{1}$$

$$I_{n+1}(t) - I_n(t) = -\left(G_n + C_n \frac{d}{dt}\right) V_n(t) + I_{\text{tt},n}(t) \tag{2}$$

where R_n is a series resistance, L_n a series inductance, G_n a shunt conductance (normally zero for a solenoid), and C_n a shunt capacitance. The remaining terms are voltage and current sources from the inter-turn couplings. While Fig. 1(b) only shows capacitive couplings between nearest neighbors, the general forms for these couplings are

$$V_{\text{tt},n} = -\sum_{j \neq n} M_{nj} \frac{d}{dt} I_j(t) \tag{3}$$

$$I_{\text{tt},n} = \sum_{j \neq n} C_{nj} \frac{d}{dt} [V_j(t) - V_n(t)] \tag{4}$$

where M_{nj} is a mutual inductance, C_{nj} is a mutual capacitance, and the sums include all other turns. These coupling coefficients are reciprocal: $M_{nj} = M_{jn}$ and $C_{nj} = C_{jn}$.

Together, Eqs. (1)–(4) form a network model for the solenoid. Rearranging terms, here are two additional ways to present the same model. The first way resembles the Telegrapher's equations with differential turn couplings for both voltage and current:

$$V_n(t) - V_{n-1}(t) = -\left(R_n + \sum_{j=1}^{N} M_{nj} \frac{d}{dt}\right) I_n(t) + \sum_{j=1}^{N} M_{nj} \frac{d}{dt} [I_n(t) - I_j(t)] \tag{5}$$

$$I_{n+1}(t) - I_n(t) = -\left(G_n + C_n \frac{d}{dt}\right) V_n(t) + \sum_{j=1}^{N} C_{nj} \frac{d}{dt} [V_j(t) - V_n(t)]. \tag{6}$$

Let's call this the "telegraph form." It's particularly convenient for approximations to come. As written, the sums are complete (as we'll need later) though some diagonal terms do not contribute. The form assumes the diagonal mutual inductances are self inductances,

$$M_{nn} = L_n, \tag{7}$$

which is a useful convention. However, it doesn't require us to define C_{nn} yet. Visually, this form suggests that the inter-turn couplings do not affect the shunt capacitance while they do contribute to the series inductance. As we'll see below, this is misleading because the usual circuit coefficient C_n already includes contributions from the other turns.

The second way is a very concise form:

$$V_n(t) - V_{n-1}(t) = -R_n I_n(t) - \sum_{j=1}^{N} M_{nj} \frac{d}{dt} I_j(t) \tag{8}$$

$$I_{n+1}(t) - I_n(t) = -G_n V_n(t) + \sum_{j=1}^{N} C_{nj} \frac{d}{dt} V_j(t). \tag{9}$$

Let's call this the "compact form." As written, the sums are complete and all terms contribute. In addition to (7), this form assumes the mutual capacitances

$$C_{nj} = -\mathbb{C}_{nj} \tag{10}$$

are negative values of the capacitance matrix $\mathbb{C}$, as described in the next section. This sets

$$\sum_j C_{nj} = -C_n \tag{11}$$

which is a useful convention.

The energy stored by the solenoid as a network is

$$\begin{aligned}
U = &\frac{1}{2} \sum_{n=1}^{N} L_n \langle I_n(t)^2 \rangle + \frac{1}{2} \sum_{n=1}^{N} \sum_{j \neq n} M_{nj} \langle I_n(t) I_j(t) \rangle \\
&+ \frac{1}{2} \sum_{n=1}^{N} C_n \langle V_n(t)^2 \rangle + \frac{1}{4} \sum_{n=1}^{N} \sum_{j \neq n} C_{nj} \langle [V_n(t) - V_j(t)]^2 \rangle \\
= &\frac{1}{2} \sum_{n=1}^{N} \sum_{j=1}^{N} M_{nj} \langle I_n(t) I_j(t) \rangle - \frac{1}{2} \sum_{n=1}^{N} \sum_{j=1}^{N} C_{nj} \langle V_n(t) V_j(t) \rangle
\end{aligned} \tag{12}$$

where brackets denote a time average. The second version follows from (7), (10), and (11).

A.   Connecting with the capacitance matrix

The coefficients C_n and C_{nj} are related to the capacitance matrix $\mathbb{C}$ of electrostatics, which has many useful properties. For background, I recommend Refs. 10 and 11. The coefficients of the capacitance matrix for a group of N conductors are defined by the relationship

$$Q_n = \sum_j \mathbb{C}_{nj} V_j \tag{13}$$

between their charges Q_n and voltages V_j. The diagonal terms $\mathbb{C}_{nn}$ are known as coefficients of capacity and are the self capacitances of each conductor when all others are grounded. The off-diagonal terms $\mathbb{C}_{nj}$ are known as coefficients of induction. Some important properties:

$$\mathbb{C}_{nj} = \mathbb{C}_{jn}, \qquad \mathbb{C}_{nn} \geq 0, \qquad \mathbb{C}_{nj} \leq 0 \ (n \neq j), \qquad \text{and} \qquad \mathbb{C}_{nn} \geq -\sum_{j \neq n} \mathbb{C}_{nj}. \qquad (14)$$

Last but not least, the convention (11) follows from the assignment $C_{nj} = -\mathbb{C}_{nj}$ of (10) and

$$\sum_{j=1}^{N} \mathbb{C}_{nj} = C_n \geq 0. \qquad (15)$$

This property is a little subtle in that it assumes the sum doesn't include a bounding conductive environment (or when there is none, an effective conductor at the point at infinity).[10] This property shows that C_n secretly includes inter-turn couplings, and with (14) that those terms reduce (shield) the value of C_n from the larger value C_{nn} that it'd be for the turn when all other turns are grounded.

We can use the capacitance matrix as long as we assume the solenoid behaves quasistatically. To make the connection clear, let Q_n be the charge of the n-th turn, which is the same as that on the top plate of C_n. Then the turn current differences

$$I_{n+1} - I_n = -G_n V_n - \frac{dQ_n}{dt}. \qquad (16)$$

Using (13), the capacitor currents

$$\frac{dQ_n}{dt} = \sum_{j=1}^{N} \mathbb{C}_{nj} \frac{dV_j}{dt} = \left(\sum_{j=1}^{N} \mathbb{C}_{nj} \right) \frac{dV_n}{dt} + \sum_{j=1}^{N} \mathbb{C}_{nj} \frac{d}{dt} [V_j(t) - V_n(t)]. \qquad (17)$$

Together, (16) and (17) with (10) and (11) recover (6).

The quasistatic energy for static potentials using the capacitance matrix is

$$U = \frac{1}{2} \sum_{n=1}^{N} Q_n V_n = \frac{1}{2} \sum_{n=1}^{N} \sum_{j=1}^{N} \mathbb{C}_{nj} V_n V_j, \qquad (18)$$

where the factor of $1/2$ comes from the work of placing the charges: $\int_0^Q qV \, dq = QV/2$. Accounting for time variation, the is the same as the capacitive part in the second version of (12), and recovers the first version using the substitution $V_n V_j = \frac{1}{2} \left[V_n^2 + V_j^2 - (V_n - V_j)^2 \right]$.

III.   CONTINUOUS APPROXIMATION

At this point, we have a network model that's suitable for numerical work but a little awkward for further exploration. To keep going, let's convert the network model to a transmission-line one by making the following connection between discrete and continuous parameters. This connection does not uniquely determine the continuous model, but instead provides a correspondence for when they should be approximately equivalent.

To proceed, let the solenoid have a height H and a uniform turn spacing $h = H/N$ (center to center). For each position x along the solenoid, let the voltage and current be $V(x,t)$ and $I(x,t)$. Then we can connect the circuit variables as

$$V_n(t) = V(x_n, t) \quad \text{and} \quad I_n(t) = I(x_n, t) \tag{19}$$

where $x_n = nh$ is an approximate location for the n-th turn.

Next, it's tempting to take a continuum limit of infinite turns ($N \longrightarrow \infty$, $h \longrightarrow 0$, H fixed). However, the finite value of h does capture the actual discrete nature of the turns, and is important in relating the discrete and continuous parameters. In other words, real solenoids likely have a hybrid mixture of discrete and continuous properties. Fortunately, we can still proceed by noting that for a large number of turns, the first-order finite differences are very nearly

$$V_n(t) - V_{n-1}(t) \approx \frac{\partial V(x_n, t)}{\partial x} h \tag{20}$$

$$I_{n+1}(t) - I_n(t) \approx \frac{\partial I(x_n, t)}{\partial x} h. \tag{21}$$

Likewise, the sums that include all terms are Riemann approximations of definite integrals,

$$h \sum_{n=0}^{N} F(x_n) \approx \int_0^H F(x) dx. \tag{22}$$

There's a subtlety in that the index n should start at $n = 0$ instead of $n = 1$, as in the network model, but for us the $n = 0$ terms have null coefficients so do not contribute.

A. Relationship between parameters

With the above approximations, we're nearly set. What's left is to relate the discrete parameters to new continuous ones. First, the core coefficients R_n, L_n, G_n, and C_n become functions $r(x), l(x), g(x)$, and $c(x)$ with units distributed per length. Using the telegraph form, the network model provides constraints for the values

$$r(x_n) \approx R_n/h, \quad l(x_n) \approx \sum_{j=1}^{N} M_{nj}/h, \quad g(x_n) \approx G_n/h, \quad \text{and} \quad c(x_n) \approx C_n/h. \tag{23}$$

Note that $l(x)$ includes the effects of inter-turn coupling as arranged in the telegraph form. Interpolating between these finite-sampled values has some freedom, but should be consistent with integrals corresponding to sums at least globally and, ideally, locally (e.g., $\int_0^H r(x)dx \approx \sum_{n=1}^{N} R_n$ and $\int_0^h r(x_n + y)dy \approx R_n$).

Next, the inter-turn coupling coefficients M_{nj} and C_{nj} become functions $m(x,y)$ and $c(x,y)$ with units distributed per length squared. Like the coefficients, these functions are symmetric: $m(x,y) = m(y,x)$ and $c(x,y) = c(y,x)$. Using the Riemann approximation (22), the network model suggests constraints for the values

$$m(x_n, x_j) \approx M_{nj}/h^2 \qquad \text{and} \qquad c(x_n, x_j) \approx C_{nj}/h^2 = -\mathbb{C}_{nj}/h^2. \tag{24}$$

Considering arbitrary voltage and current distributions, the interpolation between these values is constrained by local integrals: $\int_0^h m(x_n, x_j + y)dy \approx M_{nj}/h$ and $\int_0^h c(x_n, x_j + y)dy \approx C_{nj}/h$. Globally, their integrals are constrained to be

$$\int_0^H m(x,y)dy = l(x) \qquad \text{and} \qquad \int_0^H c(x,y)dy = -c(x), \qquad (25)$$

where the negative sign for capacitance is a property from the capacitance matrix. Interestingly, this means that $c(x,y)$ abruptly reverses sign as x and y vary from being off-diagonal to diagonal, $x = y$, where the peak values of $c(x,x)$ are located. This peak behavior of $c(x,y)$ and its sharpness are controlled (and likely blunted) by the finite value of h. Likewise, $m(x,y)$ reaches its peak values on the diagonal. For the typical case where all turns have the same winding direction, $m(x,y)$ should be positive everywhere and vary smoothly.

IV. TRANSMISSION-LINE MODEL

Using the approximations (20–22) and parameters of the last section, the network model converts to a pair of coupled integro-differential equations. The telegraph form becomes

$$\frac{\partial V(x,t)}{\partial x} = -\left(r(x) + l(x)\frac{\partial}{\partial t} \right) I(x,t) + \int_0^H m(x,y)\frac{\partial}{\partial t}[I(x,t) - I(y,t)]dy \qquad (26)$$

$$\frac{\partial I(x,t)}{\partial x} = -\left(g(x) + c(x)\frac{\partial}{\partial t} \right) V(x,t) + \int_0^H c(x,y)\frac{\partial}{\partial t}[V(y,t) - V(x,t)]dy \qquad (27)$$

and the compact form becomes

$$\frac{\partial V(x,t)}{\partial x} = -r(x)I(x,t) - \int_0^H m(x,y)\frac{\partial I(y,t)}{\partial t}dy \qquad (28)$$

$$\frac{\partial I(x,t)}{\partial x} = -g(x)V(x,t) + \int_0^H c(x,y)\frac{\partial V(y,t)}{\partial t}dy. \qquad (29)$$

Likewise, the energy stored by the solenoid becomes

$$U = \frac{1}{2}\iint_0^H m(x,y)\langle I(x,t)I(y,t)\rangle dxdy - \frac{1}{2}\iint_0^H c(x,y)\langle V(x,t)V(y,t)\rangle dxdy, \qquad (30)$$

where the minus sign for the capacitive term follows from the capacitance matrix.

This model seems to agree with that used in numerical work by the TSSP [c.f., Ref. 4: Eqs. (4.16) and (4.17) of pn2511 and Eqs. (2.1) and (2.2) of pn1401]. There is a minor difference in that the TSSP separated $c(x,y)$ into internal (off-diagonal) and external (diagonal) functions, while we merged them following the capacitance matrix. Additionally, TSSP includes some extra features to model the secondary coil of a Tesla transformer. We could add most of them by treating a top capacitive load (toroid electrode) as an extra $(n = N + 1)$ turn and manually adding an inductive coupling with a primary coil. The pn2511 document (c.f., Fig. 6.1) has an interesting discussion of how (27) usually predicts an internal point of maximum current for the fundamental resonant mode in Tesla transformers.

A. Notes on decoupling the equations

The classic Telegrapher's equations for a uniform transmission line without inter-turn coupling integrals are straightforward to decouple into equations for only voltage or current. This follows by taking a spatial derivative of one equation and substituting in the other, which gives

$$\frac{\partial^2 V(x,t)}{\partial x^2} = \left(r + l\frac{\partial}{\partial t}\right)\left(g(x) + c(x)\frac{\partial}{\partial t}\right)V(x,t) \tag{31}$$

$$\frac{\partial^2 I(x,t)}{\partial x^2} = \left(r(x) + l(x)\frac{\partial}{\partial t}\right)\left(g + c\frac{\partial}{\partial t}\right)I(x,t). \tag{32}$$

If the coefficients are uniform, the equations are the same for voltage and current. If some coefficients are nonuniform then this approach doesn't work simultaneously for both voltage and current, but instead may work for one or the other as indicated above. Here and subsequently, r, l, g, and c are the values of $r(x), l(x), g(x)$, and $c(x)$ if they are uniform.

For a solenoid, though, it doesn't seem that there's a general way to decouple the equations. It's tempting to try integration by parts with the integrals to introduce spatial derivatives, but this seems to be blocked by the antiderivatives of $m(x,y)$ and $c(x,y)$ being constant with respect to the variable of integration. However, decoupling is straightforward later using some approximations.

V. SIMPLIFIED TRANSMISSION-LINE MODELS

Next, let's consider various approximations of the transmission-line model.

A. Long-wavelength approximation (lumped regime)

In the long-wavelength regime, the solenoid should behave like a simple lumped circuit element. There are two straightforward cases that follow from the telegraph form. The first case has spatially uniform current $I(x,t) = I_0(t)$. In this one, integrating (26) gives the usual result for series conduction through a lumped inductor

$$V(H,t) - V(0,t) = -\left(R_0 + L_0\frac{d}{dt}\right)I_0(t) \tag{33}$$

with total series resistance and inductance

$$R_0 = \int_0^H r(x)dx = \sum_{n=1}^N R_n \tag{34}$$

$$L_0 = \int_0^H l(x)dx = \sum_{n=1}^N \sum_{j=1}^N M_{nj}. \tag{35}$$

The voltage equation of the telegraph or compact form provide a consistency check for the actual voltage profile that likely cannot be satisfied in general unless $g(x) = c(x) = 0$ or a nonuniform current is allowed.

However, the stored energy (30) can be used to estimate an appropriate capacitance from the voltage profile as

$$C_U = -\iint_0^H c(x,y)\langle V(x,t)V(y,t)\rangle dxdy \Big/ \left\langle [V(H,t) - V(0,t)]^2 \right\rangle. \tag{36}$$

For the special case of a linear voltage profile $V(x,t) = V_0(t)(x/H)$, this reduces to

$$C_U = -\iint_0^H c(x,y)x\,y\,dxdy/H^2. \tag{37}$$

We can simplify this further with the substitution $xy = [x^2 + y^2 - (x-y)^2]/2$, giving

$$C_U = \int_0^H c(x)x^2 dx/H^2 + \iint_0^H c(x,y)(x-y)^2 dxdy/(2H^2) \gtrsim \int_0^H c(x)x^2 dx/H^2. \tag{38}$$

The lower bound should be a decent approximation because the factor of $(x-y)^2$ in the neglected integral should sharply suppress the dominant content in $c(x,y)$ located about $x = y$. There's a subtlety in showing that this is a lower bound because of the change in sign of $c(x,y)$ in a finite region of width h about this diagonal, but appealing to the original network model and its energy (12) clears this up. This is shown later for the local-coupling approximation, which introduces an elastance $\mathcal{S}_{tt}^{(2)}(x)$ such that

$$\iint_0^H c(x,y)(x-y)^2 dxdy/(2H^2) = \frac{1}{2H^2} \int_0^H \frac{1}{\mathcal{S}_{tt}^{(2)}(x)} dx \geq 0. \tag{39}$$

For the particularly special case of a nearly uniform $c(x) \approx c$, the lower bound reduces to

$$C_U \approx \frac{1}{3}C_0 \tag{40}$$

for $C_0 = cH$ as defined below. I've called this the Miller self-capacitance of a solenoid inductor in previous notes that derived it from modeling a Tesla transformer or tested it with an actual solenoid.[2,3] There's an improved estimate

$$C_U \approx \frac{1}{3}C_0 + \frac{1}{2H^2} \int_0^H \frac{1}{\mathcal{S}_{tt}^{(2)}(x)} dx \approx \frac{1}{3}C_0 + \frac{1}{2\,\bar{\mathcal{S}}_{tt}^{(2)}H} \tag{41}$$

from adding back the other integral and optionally using the infinite-line approximation.

The second case has spatially uniform voltage $V(x,t) = V_0(t)$. In this case, integrating (27) gives the usual result for parallel conduction across a wire tapped by a lumped capacitor shunted to ground that steals some current

$$I(H,t) - I(0,t) = -\left(G_0 + C_0\frac{d}{dt}\right)V_0(t) \tag{42}$$

with total shunt conductance and capacitance

$$G_0 = \int_0^H g(x)dx = \sum_{n=1}^N G_n \tag{43}$$

$$C_0 = \int_0^H c(x)dx = \sum_{n=1}^N C_n. \tag{44}$$

Again, the current equation of the telegraph or compact form provides a consistency check for the actual current profile that likely cannot be satisfied in general unless $r(x) = l(x) = 0$ or a nonuniform voltage is allowed.

The stored energy (30) can be used to estimate an appropriate inductance from the current profile as

$$L_U = \iint_0^H m(x,y)\langle I(x,t)I(y,t)\rangle dxdy \Big/ \langle I(x_0,t)^2\rangle, \tag{45}$$

which is of a similar form as the capacitance C_U above but references the current at one position x_0. In the special case of a linear current profile $I(x,t) = I_0(t)(x/H)$, say from the solenoid acting as a capacitor fed from its top by a voltage source with its bottom left open circuit, then you can use the same tricks to show that

$$L_U = \iint_0^H m(x,y)x\,y\,dxdy/H^2 = \int_0^H l(x)x^2 dx/H^2 - \iint_0^H m(x,y)(x-y)^2 dxdy/(2H^2) \tag{46}$$

$$\lesssim \int_0^H l(x)x^2 dx/H^2. \tag{47}$$

Here, the lower bound assumes $m(x,y)$ is everywhere positive, which is normally true (uniform winding direction). Again, for the particularly special case of a nearly uniform $l(x) \approx l$, this reduces to

$$L_U \approx \frac{1}{3}L_0 \tag{48}$$

for $L_0 = lH$ as defined above. We could call this the Miller self-inductance of a capacitor because the same person also derived this for antennas over 100 years ago.[12] Later, the local-coupling approximation will introduce a reluctance $\mathcal{R}_{tt}^{(2)}(x)$ such that

$$\iint_0^H m(x,y)(x-y)^2 dxdy/(2H^2) = \frac{1}{2H^2}\int_0^H \frac{1}{\mathcal{R}_{tt}^{(2)}(x)}dx \geq 0, \tag{49}$$

where positivity assumes the winding direction is the same for all turns. This gives an improved estimate

$$L_U \approx \frac{1}{3}L_0 - \frac{1}{2H^2}\int_0^H \frac{1}{\mathcal{R}_{tt}^{(2)}(x)}dx \approx \frac{1}{3}L_0 - \frac{1}{2\bar{\mathcal{R}}_{tt}^{(2)}H} \tag{50}$$

from adding back the other integral and optionally using the infinite-line approximation.

Please see Ref. 13 for a treatment of linear profiles that are not zero at one end.

B. Local-coupling approximation (converting integrals to derivatives)

At a place x along the solenoid that is far enough from the ends to not be influenced much by them, the solenoid looks roughly like an infinitely long transmission line. Over a region like this with properties that vary slowly or not at all with position, it seems reasonable to wonder if there's a way to simplify the inter-turn couplings to be more local. It turns out there is a way to do this, by converting the global coupling integrals to sums of local higher-order derivatives. This works for a finite line as treated here, and simplifies for a nearly infinite line as shown in the next section.

Consider the telegraph form of the transmission-line model. Let's assume our current and voltage functions are well behaved enough to use a Taylor-series expansion such as

$$V(y,t) \approx \sum_{p=0}^{\infty} \frac{(y-x)^p}{p!} \frac{\partial^p V(x,t)}{\partial x^p}. \tag{51}$$

Then, looking at the voltage inter-turn integral (ignoring a time derivative), we have

$$\int_0^H c(x,y)[V(y,t) - V(x,t)]dy \approx \sum_{p=1}^{\infty} \left[\frac{1}{p!} \int_0^H c(x,y)\,(y-x)^p dy \right] \frac{\partial^p V(x,t)}{\partial x^p}. \tag{52}$$

Here, approximate signs warn that in general the series could potentially fail and that, numerically, things could get interesting especially with truncation.

For the capacitive couplings, the series coefficients are position-dependent series distributed elastances (reciprocal capacitances)

$$\frac{1}{\mathcal{S}_{\text{tt}}^{(p)}(x_n)} = \frac{1}{p!} \int_0^H c(x_n,y)\,(y-x_n)^p \, dy \approx \frac{1}{p!h} \sum_{j=1}^{N} C_{nj}[(j-n)h]^p \tag{53}$$

for positive integers $p = 1, 2, 3, \ldots$, because each $\mathcal{S}_{\text{tt}}^{(p)}$ has units of Farad^{-1} meter^{1-p}. (The first with $p = 1$, though, isn't distributed.) The coefficient $\mathcal{S}_{\text{tt}}^{(2)}(H/2)$ has a simple interpretation in the next section. The same approach works also for the current inter-turn integrals. There, the series coefficients are position-dependent series distributed reluctances (reciprocal inductances)

$$\frac{1}{\mathcal{R}_{\text{tt}}^{(p)}(x_n)} = \frac{1}{p!} \int_0^H m(x_n,y)\,(y-x_n)^p \, dy \approx \frac{1}{p!h} \sum_{j=1}^{N} M_{nj}[(j-n)h]^p. \tag{54}$$

Together, these new elastances and reluctances are properties of the solenoid. For even p the coefficients are positive, but for odd p the coefficients can be positive or negative, depending on position. (Positive reluctances here assume a single winding direction.) These coefficients do not seem to converge for an infinitely long solenoid, so they are really only defined for a finite length H. This probably follows from our quasistatic, lumped-circuit approach that assumes all inter-turn couplings act instantaneously, no matter how distant.

Using these new coefficients, the transmission-line model becomes

$$\frac{\partial V(x,t)}{\partial x} \approx -\left[r(x) + \left(l(x) + \sum_{p=1}^{\infty} \frac{1}{\mathcal{R}_{\text{tt}}^{(p)}(x)} \frac{\partial^p}{\partial x^p} \right) \frac{\partial}{\partial t} \right] I(x,t) \tag{55}$$

$$\frac{\partial I(x,t)}{\partial x} \approx -\left[g(x) + \left(c(x) - \sum_{p=1}^{\infty} \frac{1}{\mathcal{S}_{\text{tt}}^{(p)}(x)} \frac{\partial^p}{\partial x^p} \right) \frac{\partial}{\partial t} \right] V(x,t). \tag{56}$$

Let's call this the local-coupling approximation. Following the same steps as above, the energy (30) becomes

$$U \approx \frac{1}{2} \int_0^H l(x) \langle I(x,t)^2 \rangle dx + \frac{1}{2} \sum_{p=1}^{\infty} \int_0^H \frac{1}{\mathcal{R}_{\text{tt}}^{(p)}(x)} \left\langle I(x,t) \frac{\partial^p I(x,t)}{\partial x^p} \right\rangle dx$$

$$+ \frac{1}{2} \int_0^H c(x) \langle V(x,t)^2 \rangle dx - \frac{1}{2} \sum_{p=1}^{\infty} \int_0^H \frac{1}{\mathcal{S}_{\text{tt}}^{(p)}(x)} \left\langle V(x,t) \frac{\partial^p V(x,t)}{\partial x^p} \right\rangle dx. \tag{57}$$

Note that the above expressions include both even and odd p terms. The dominant terms are expected to be the even terms, as discussed in the next section, with coefficients that reduce to roughly half their values near the edges. The odd terms are expected to be most important near the edges, but highly suppressed in the interior.

Though it doesn't look like it, (57) does agree with the results of the last section that used $\mathcal{S}_{\text{tt}}^{(2)}(x)$ or $\mathcal{R}_{\text{tt}}^{(2)}(x)$ for the special case of a linear gradient. For example, for $V(x,t) = V_0(t)(x/H)$, the straightforward result produces a term with $-\int_0^H x[\mathcal{S}_{\text{tt}}^{(1)}(x)]^{-1}dx$ instead of $\int_0^H [\mathcal{S}_{\text{tt}}^{(2)}(x)]^{-1}dx$. However, using $(y-x)^p = -[(-1)^p y(x-y)^{p-1} + x(y-x)^{p-1}]$ with the symmetry $c(x,y) = c(y,x)$, you can show that those are equivalent, giving in general

$$\int_0^H \frac{1}{\mathcal{S}_{\text{tt}}^{(p)}(x)} dx = \frac{-[(-1)^p + 1]}{p} \int_0^H \frac{x}{\mathcal{S}_{\text{tt}}^{(p-1)}(x)} dx. \tag{58}$$

The same relation holds for the reluctances.

Finally, note that the network model can also be modified similarly to use higher-order finite differences.[14] However, numerically computing higher-order finite differences seems less straightforward than just doing the original sums.

C. Nearly infinite-line approximation (simplifying terms)

Building on the local-coupling approximation of the last section, assume the solenoid is long enough such that within an interior region of interest the edges can be safely ignored, as if they're infinitely far away. Assume also that within this region the solenoid is approximately translationally invariant (locally uniform). Then the inter-turn coupling coefficients are independent of position x within this region, at least approximately, and reduce to

$$M_{(\delta)} = M_{(-\delta)} \approx M_{n,n+\delta} = M_{n+\delta,n} \approx M_{n,n-\delta} = M_{n-\delta,n} \tag{59}$$

$$C_{(\delta)} = C_{(-\delta)} \approx C_{n,n+\delta} = C_{n+\delta,n} \approx C_{n,n-\delta} = C_{n-\delta,n} \tag{60}$$

for the network model using an inter-turn distance index δ and likewise

$$c_{(\delta)}(x-y) = c_{(\delta)}(y-x) \approx c(x, x+y) = c(x+y, x) \approx c(x, x-y) = c(x-y, x) \tag{61}$$

$$m_{(\delta)}(x-y) = m_{(\delta)}(y-x) \approx m(x, x+y) = m(x+y, x) \approx m(x, x-y) = m(x-y, x) \tag{62}$$

for the transmission-line model, where the subscript "(δ)" only indicates this approximation.

Using these, the elastances and reluctances of the last section are then

$$\frac{1}{\mathcal{S}_{\rm tt}^{(p)}(x_n)} = \frac{1}{p!} \int_{-x_n}^{H-x_n} c_{(\delta)}(y)\, y^p \, dy \approx \frac{1}{p!h} \sum_{\delta=-n}^{N-n} C_{(\delta)}(\delta h)^p \tag{63}$$

$$\frac{1}{\mathcal{R}_{\rm tt}^{(p)}(x_n)} = \frac{1}{p!} \int_{-x_n}^{H-x_n} m_{(\delta)}(y)\, y^p \, dy \approx \frac{1}{p!h} \sum_{\delta=-n}^{N-n} M_{(\delta)}(\delta h)^p, \tag{64}$$

which is a different way of presenting the same results.

However, given our assumptions, these functions should be nearly independent of position. They should be well approximated by their values at the center of the solenoid,

$$\frac{1}{\bar{\mathcal{S}}_{\rm tt}^{(p)}} = \frac{1}{\mathcal{S}_{\rm tt}^{(p)}(H/2)} = \frac{1+(-1)^p}{p!} \int_0^{H/2} c_{(\delta)}(y)\, y^p dy \approx \frac{1+(-1)^p}{p!h} \sum_{\delta=1}^{N/2} C_{(\delta)}(\delta h)^p \geq 0 \tag{65}$$

$$\frac{1}{\bar{\mathcal{R}}_{\rm tt}^{(p)}} = \frac{1}{\mathcal{R}_{\rm tt}^{(p)}(H/2)} = \frac{1+(-1)^p}{p!} \int_0^{H/2} m_{(\delta)}(y)\, y^p dy \approx \frac{1+(-1)^p}{p!h} \sum_{\delta=1}^{N/2} M_{(\delta)}(\delta h)^p \geq 0, \tag{66}$$

which are positive for even p and zero for odd p. That is, far from the edges, the odd p terms are highly suppressed. Again, note that these values do depend on H and likely do not converge for infinite H.

The first nonzero $\mathcal{S}_{\rm tt}^{(2)}(H/2)$ is related with the total capacitance formed by the network of inter-turn capacitances: $\sum_{\delta=1}^{N} \delta\, C_{(\delta)}/(N/\delta) \approx \sum_{\delta=1}^{N/2} C_{(\delta)}\delta^2/N = 1/\left[\bar{\mathcal{S}}_{\rm tt}^{(2)} H\right]$. This assumes the high-order contributions for $\delta \gtrsim N/2$ are negligible and, as above, cavalierly uses $N/2$ as an upper bound for sums.

Using these new coefficients, the transmission-line model becomes

$$\frac{\partial V(x,t)}{\partial x} \approx -\left[r + \left(l + \sum_{p=1}^{\infty} \frac{1}{\bar{\mathcal{R}}_{\rm tt}^{(2p)}} \frac{\partial^{2p}}{\partial x^{2p}}\right) \frac{\partial}{\partial t}\right] I(x,t) \tag{67}$$

$$\frac{\partial I(x,t)}{\partial x} \approx -\left[g + \left(c - \sum_{p=1}^{\infty} \frac{1}{\bar{\mathcal{S}}_{\rm tt}^{(2p)}} \frac{\partial^{2p}}{\partial x^{2p}}\right) \frac{\partial}{\partial t}\right] V(x,t). \tag{68}$$

Let's call this the (nearly) infinite-line approximation. Likewise, the energy (57) becomes

$$U \approx \frac{1}{2} l \int_0^H \langle I(x,t)^2 \rangle dx + \frac{1}{2} \sum_{p=1}^{\infty} \frac{1}{\bar{\mathcal{R}}_{\rm tt}^{(2p)}} \int_0^H \left\langle I(x,t) \frac{\partial^{2p} I(x,t)}{\partial x^{2p}} \right\rangle dx$$

$$+ \frac{1}{2} c \int_0^H \langle V(x,t)^2 \rangle dx - \frac{1}{2} \sum_{p=1}^{\infty} \frac{1}{\bar{\mathcal{S}}_{\rm tt}^{(2p)}} \int_0^H \left\langle V(x,t) \frac{\partial^{2p} V(x,t)}{\partial x^{2p}} \right\rangle dx, \tag{69}$$

which only has even order terms. This only works within the region of interest, far from the edges.

D. Neglecting all but capacitances between neighboring turns

There's a special case of the infinite-line approximation that appears in Refs. 5–9. This case focuses on the capacitive couplings between nearest-neighbor turns and otherwise assumes a uniform transmission line. Using the last section's results, this gives

$$\frac{\partial V(x,t)}{\partial x} \approx - \left[r + l\frac{\partial}{\partial t} \right] I(x,t) \tag{70}$$

$$\frac{\partial I(x,t)}{\partial x} \approx - \left[g + \left(c - \frac{1}{\bar{\mathcal{S}}_{tt,1}^{(2)}} \frac{\partial^2}{\partial x^2} \right) \frac{\partial}{\partial t} \right] V(x,t) \tag{71}$$

which is a uniform line with the first elastance term kept. However, in this case, the elastance coefficient is slightly different, in that it accounts only for the coupling between neighboring turns: $\bar{\mathcal{S}}_{tt}^{(2)} \approx \bar{\mathcal{S}}_{tt,1}^{(2)} = 1/(C_{(1)}h)$. Refs. 6–8 call this coefficient the series-capacitance parameter and dive into estimating and measuring it. Ref. 5 pointed out that it's an elastance, which is what tipped me off to call the new coefficients in the last two sections elastances and reluctances. (Both are neat examples of the many delightful electromagnetic terms coined by Oliver Heaviside.) The model of Ref. 9, given by its Eqs. (25) and (33), is an improvement that combines (71) from above with the more general (28) from before.

This minimal model is likely the simplest approximation that adds in some of the effects of non-ideal capacitances in a solenoid inductor. As we'll see later, it predicts a high-frequency cutoff (and a low-frequency cutoff if $r, g \neq 0$), which might not occur in practice (discussed below).[30] Note that this model follows directly from the network model because

$$\sum_{j=1}^{N} C_{nj}[V_j(t) - V_n(t)] \approx C_{(1)}[V_{n-1}(t) + V_{n+1}(t) - 2V_n(t)] \approx C_{(1)}\frac{\partial^2 V(x_n,t)}{\partial x^2} h^2, \tag{72}$$

using the definition of a second-order centered finite difference.[14]

E. Harmonic-signal approximation (spatial Fourier transform)

Consider voltages and currents that are proportional to $\exp(ikx)$ just like typical spatial-harmonic waves on uniform transmission lines. For traveling waves, the sign of k indicates direction ($k = \pm|k|$ propagates towards $\pm\hat{x}$ for an $e^{-i\omega t}$ time dependence). Assuming this form of solution, we could simplify things by direct substitution or by using the local-coupling or infinite-line approximations. However, there are some subtleties with consistency, because generally such solutions are coupled by the model. To proceed, let's use Fourier transforms[15] to safely explore and then return to substitution and those approximations.

Let's use Fourier transforms[15] with the convention

$$\mathcal{F}[P(t)](k) = \int_{-\infty}^{\infty} P(x,t)e^{-ikx}dx \tag{73}$$

where $P(x,t)$ is an arbitrary function, $\mathcal{F}[P(t)](k)$ is its spectrum, and k is a wavenumber. The inverse is $P(x,t) = (2\pi)^{-1}\int_{-\infty}^{\infty}\mathcal{F}[P(t)](k)e^{ikx}dk$. Some transforms[15] we'll need are

$$\mathcal{F}[\partial P(t)/\partial x](k) = ik\,\mathcal{F}[P(t)](k) \tag{74}$$

$$\mathcal{F}[P_1 P_2](k) = (\mathcal{F}[P_1] * \mathcal{F}[P_2])(k)/(2\pi) \tag{75}$$

$$\mathcal{F}[(P_1 * P_2)](k) = \mathcal{F}[P_1](k)\mathcal{F}[P_2](k) \tag{76}$$

$$\mathcal{F}[e^{ik_0 x}](k) = 2\pi\delta(k - k_0) \tag{77}$$

where $\delta(x)$ is a Diract delta function and the star notation means a convolution of the form

$$(P_1 * P_2)(x) = \int_{-\infty}^{\infty} P_1(x - y)P_2(y)dy. \tag{78}$$

To use these, treat the voltages and currents as if they have infinite domain ($x \in [-\infty, \infty]$) and set the coupling parameters to zero outside the solenoid ($x \notin [0, H]$).

Starting with the compact form of the transmission-line model, there's no obvious way to decouple solutions with different values of k. However, note that if we follow the setup of the infinite-line approximation, then the coupling integrals are convolutions:

$$\int_0^H c(x,y)V(y,t)dy \approx \int_0^H c_{(\delta)}(x-y)V(y,t)dy \approx \int_{-\infty}^{\infty} c_{(\delta)}(x-y)V(y,t)dy, = [c_{(\delta)} * V(t)](x). \tag{79}$$

Then, taking the transform of the compact form gives

$$ik\,\mathcal{F}[V(t)](k) \approx -\frac{1}{2\pi}(\mathcal{F}[r] * \mathcal{F}[I(t)])(k) - \mathcal{F}[m_{(\delta)}](k)\frac{\partial}{\partial t}\mathcal{F}[I(t)](k) \tag{80}$$

$$ik\,\mathcal{F}[I(t)](k) \approx -\frac{1}{2\pi}(\mathcal{F}[g] * \mathcal{F}[V(t)])(k) + \mathcal{F}[c_{(\delta)}](k)\frac{\partial}{\partial t}\mathcal{F}[V(t)](k). \tag{81}$$

This shows that the inter-turn couplings are now decoupled, but that any spatial dependence in $r(x)$ or $g(x)$ generally leads to couplings between different values of k. If we assume those loss coefficients are uniform, then the equations are fully decoupled:

$$ik\,\mathcal{F}[V(t)](k) \approx -r\mathcal{F}[I(t)](k) - \mathcal{F}[m_{(\delta)}](k)\frac{\partial}{\partial t}\mathcal{F}[I(t)](k) \tag{82}$$

$$ik\,\mathcal{F}[I(t)](k) \approx -g\mathcal{F}[V(t)](k) + \mathcal{F}[c_{(\delta)}](k)\frac{\partial}{\partial t}\mathcal{F}[V(t)](k). \tag{83}$$

This is the Fourier transform of the infinite-line approximation, showing that it is decoupled for spatial harmonic solutions.

To clean things up a bit, let the circuit variables have the form

$$V(x,t) = V(t)e^{ikx} \qquad \text{and} \qquad I(x,t) = I(t)e^{ikx}. \tag{84}$$

Then using these with the above result and integrating out the delta functions gives

$$ik\,V(t) \approx -\left[r + l(k)\frac{\partial}{\partial t}\right]I(t) \tag{85}$$

$$ik\,I(t) \approx -\left[g + c(k)\frac{\partial}{\partial t}\right]V(t), \tag{86}$$

where the effective distributed inductance and capacitance parameters are

$$l(k) = \mathcal{F}[m_{(\delta)}](k) = \int_{-\infty}^{\infty} m_{(\delta)}(x)e^{-ikx}dx \tag{87}$$

$$c(k) = -\mathcal{F}[c_{(\delta)}](k) = -\int_{-\infty}^{\infty} c_{(\delta)}(x)e^{-ikx}dx. \tag{88}$$

Let's call this the harmonic-signal approximation. Note that it is equivalent to the infinite-line approximation and rests on its same assumptions. In fact, using the series $e^x = \sum_{p=0}^{\infty} x^p/p!$ and truncating the domains of $c_{(\delta)}(x)$ and $m_{(\delta)}(x)$ to $x \in [-H/2, H/2]$ gives

$$l(k) = l + \sum_{p=1}^{\infty} \frac{(-1)^p k^{2p}}{\bar{\mathcal{R}}_{\text{tt}}^{(2p)}} = l - \frac{k^2}{\bar{\mathcal{R}}_{\text{tt}}^{(2)}} + \frac{k^4}{\bar{\mathcal{R}}_{\text{tt}}^{(4)}} - \dots \tag{89}$$

$$c(k) = c - \sum_{p=1}^{\infty} \frac{(-1)^p k^{2p}}{\bar{\mathcal{S}}_{\text{tt}}^{(2p)}} = c + \frac{k^2}{\bar{\mathcal{S}}_{\text{tt}}^{(2)}} - \frac{k^4}{\bar{\mathcal{S}}_{\text{tt}}^{(4)}} + \dots, \tag{90}$$

connecting this with the results of the infinite-line approximation after substitution.

If we assume a time dependence of the form $V(t), I(t) \propto e^{-i\omega t}$, then this harmonic-signal approximation gives a dispersion relation $\omega(k)$. Substitution and decoupling gives the quadratic equation $-k^2 = [r - i\omega\, l(k)][g - i\omega\, c(k)]$, whose solutions are

$$\omega(k) = -\frac{i}{2}\left(\frac{r}{l(k)} + \frac{g}{c(k)}\right) \pm \sqrt{\frac{k^2}{l(k)c(k)} - \frac{1}{4}\left(\frac{r}{l(k)} + \frac{g}{c(k)}\right)^2}. \tag{91}$$

Ignoring losses, the dispersion relation simplifies to

$$\omega(k) = \frac{\pm k}{\sqrt{l(k)c(k)}}. \tag{92}$$

For the special case of the last section, this simplifies to

$$\omega(k) = \frac{\pm k}{\sqrt{l\left(c + k^2/\bar{\mathcal{S}}_{\text{tt},1}^{(2)}\right)}}, \tag{93}$$

which has a high frequency cutoff of $|\omega(k)| \leq |\omega(\infty)| = \sqrt{\bar{\mathcal{S}}_{\text{tt},1}^{(2)}/l}$, about which the turns resonate and above which azimuthal symmetry presumably breaks for propagation.

Finally, note that you can recover the results of the local-coupling approximation using direct substitution. From the compact form, this follows from

$$\int_0^H m(x,y)I(y,t)dy = I(x,t)\, e^{-ikx} \int_0^H m(x,y)e^{iky}dy$$

$$= I(x,t) \int_0^H m(x,y)\{\cos[k(y-x)] + i\sin[k(y-x)]\}dy, \tag{94}$$

and from the telegraph form, from $e^{ikx} - e^{iky} = e^{ikx}\{1 - \cos[k(y-x)] - i\sin[k(y-x)]\}$. Using Taylor series for sine and cosine, the sine parts lead to the odd p terms and the cosine

parts to the even p terms. However, there will in general be couplings between different values of k using the local-coupling approximation, so some care is needed using substitution directly. To show that this is consistent with the harmonic-signal approximation, note that

$$e^{-ikx} \int_0^H m(x,y)e^{iky}dy \approx \int_{-\infty}^{\infty} m_{(\delta)}(x-y)e^{-ik(x-y)}dy = \mathcal{F}[m_{(\delta)}](k) \tag{95}$$

following the assumptions of the infinite-line approximation.

F. Uniform-line approximation discussion

All together, the last sections suggest that a uniform-line approximation with constant coefficients is reasonable when the (nearly) infinite-line approximation applies and you're interested in a narrow wavelength (frequency) range below the first cutoff and away from significant dispersion, such as the small-k regime or a narrow region about a specific k value. Otherwise, you have to have some reason to neglect edge effects or to expect to have weak inter-turn couplings (say, relatively suppressed by a coaxial ground sheath as in Ref. 3). All of this isn't really surprising, though, because the infinite-line approximation basically is an appeal to Floquet theory. That said, it was fun to dig in to many of the details.

VI. ESTIMATING LINE PARAMETERS

For convenience, here are notes on estimating parameters for a solenoid that's a right cylindrical winding of single-strand wire with N turns, diameter (center-to-center) D, height (edge-to-edge) H, turn spacing (center-to-center) $h = H/N$, and winding pitch angle

$$\psi \approx \arctan[h/(\pi D)] \tag{96}$$

with respect to a circumference ($\phi = 0$ for $N \longrightarrow \infty$).

A. Resistances

Roughly speaking, the resistance $r(x)$ should be decently uniform except right near the edges. The value $r(x) \approx r$ can be estimated from measurements of R_0 with an LCR meter or by using wire property tables and empirical frequency corrections. Measurements of R_0 for an example solenoid with properties given in Refs. 3 and 16 showed little to no variation from 100 to 10,000 Hz. Frequency corrections include skin and proximity effects, and rough estimates for single-layer solenoids can be found in textbooks like Ref. 17 or older radio engineering textbooks. For much more on all of this, see Ref. 18. The tape helix model provides an estimate of $r(k)$ that is supposed to match traveling-wave tube applications well (c.f., Ref. 24).

B.   Inductances

Here are some ways to analytically estimate L_0, M_{nj}, $l(x)$, $m(x, y)$, $l(k)$, $\mathcal{R}_{\mathrm{tt}}^{(2p)}(x)$, and $\bar{\mathcal{R}}_{\mathrm{tt}}^{(2p)}$. For more precise work, there are programs available like FEMM and FastHenry to estimate M_{nj}. For a deep dive on inductance calculations, see Refs. 19–21. In general, the inductance $l(x)$ should be roughly uniform in the center of the solenoid but decrease near the edges. For plots of numerical examples of $m(x, y)$, see Fig. 3.1 of TSSP pn2511.[4]

For the uniform-current self inductance L_0 of the solenoid, the standard result for an ideal, infinitely long solenoid with a non-magnetic core is

$$L_0 \approx L_\infty = \mu_0 \pi N^2 D^2 / (4H) \tag{97}$$

where μ_0 is the vacuum permeability. For a real solenoid, the Wheeler formula

$$L_0 \approx L_{\mathrm{Wheeler}} = \mu_0 \pi N^2 D^2 / (4H + 1.8D) \tag{98}$$

is more accurate. Even more accuracy is possible using the magnetostatic approach below, and a particularly simple "handbook" formula for the result is available in Ref. 22. Interestingly, $L_0 \propto N^2$ follows from the majority of the self inductance coming from the mutual inductances M_{nj} with $n \neq j$. This is also why $l(x)$ decreases near the edges (there, half the solenoid's missing). Measurements of L_0 for an example solenoid with properties given in Refs. 3 and 16 showed little to no variation from 100 to 100,000 Hz.

Magnetostatics provides an estimate for M_{nj}, ignoring eddy currents. Using Ref. 23 (c.f., pp. 192-3, Eqs. (10-16)], the mutual inductance between two coaxial circular loops of radii a and b spaced an axial distance d apart is

$$M(a, b, d) = \mu_0 \sqrt{ab}\,(2/q) \left[(1 - q^2/2)K(q) - E(q) \right] \quad \text{where} \quad q^2 = \frac{4ab}{d^2 + (a + b)^2} \tag{99}$$

and the complete elliptic integrals of the first and second kind are

$$K(x) = \int_0^{\pi/2} \frac{d\phi}{\sqrt{1 - x^2 \sin^2 \phi}}. \quad \text{and} \quad E(x) = \int_0^{\pi/2} \sqrt{1 - x^2 \sin^2 \phi}\, d\phi. \tag{100}$$

(In Mathematica, $K(x)$ is EllipticK[x^2] and $E(x)$ is EllipticE[x^2].) This provides an estimate

$$M_{nj} = M[D/2, (D - h)/2, h(n - j)] \tag{101}$$

that uses h following the approach of Ref. 23 to avoid failure when $a = b$ for the self inductance. For thin wires, this gives the usual result

$$L_n = M_{nn} \approx M[D/2, (D - h)/2, 0] \approx \mu_0 (D/2) \left[\ln(8D/h) - 2 \right]. \tag{102}$$

This approach is consistent with the ideal and Wheeler values for L_0, and could be used to estimate $l(x)$, $m(x, y)$, $l(k)$, $\mathcal{R}_{\mathrm{tt}}^{(2p)}(x)$, and $\bar{\mathcal{R}}_{\mathrm{tt}}^{(2p)}$.

The sheath helix model[24,25] provides an estimate of the harmonic case

$$l(k) \approx \frac{\mu_0 I_1(kD/2)K_1(kD/2)}{2\pi \tan(\psi)^2} \approx \frac{2L_\infty}{H} I_1(kD/2)K_1(kD/2), \tag{103}$$

for a non-magnetic core with $H = \infty$, where $I_n(x)$ and $K_n(x)$ are modified Bessel functions of the first and second kind, respectively. (If I haven't goofed the transcription.) Numerically, $l(k) = L_\infty/H$ for small k and then decreases monotonically as k grows. Using Mathematica, expanding in k readily gives a series in even powers of kD,

$$l(k) \approx \frac{L_\infty}{H} \left\{ 1 + 0.1250 \left[\ln(kD) - 1.059\right](kD)^2 + 0.007813 \left[\ln(kD) - 1.642\right](kD)^4 + \ldots \right\},$$
(104)

and each coefficient for the k^{2p} term provides an estimate of $\bar{\mathcal{R}}_{\mathrm{tt}}^{(2p)}$.

It's interesting to note that you could significantly alter things by changing the winding direction of some turns or patches of turns, such as in a "folded" helix. For example, alternating the winding direction with each turn (which is a little impractical) would significantly impact all magnetic properties and reduce L_0.

C.   Capacitances

Here are some ways to estimate C_0, $c(k)$, and $\bar{\mathcal{S}}_{\mathrm{tt}}^{(2)}$. Otherwise, programs like FastCap and FEMM can provide estimates of C_{nj} and thus most everything else. In general, the capacitance $c(x)$ should be roughly uniform in the center of the solenoid, but increase near the edges (unless there's shielding by nearby conductors to reduce this). For a deep dive, note that it's estimation is related to the surprisingly difficult problem of finding the charge density on a thin straight wire.[26] For plots of numerical examples of $c(x)$ and $c(x,y)$, see Figs. 2.2 and 2.4 of TSSP pn2511.[4]

For the uniform-voltage self capacitance C_0 of a finite solenoid, two standard results[27] are

$$C_0 \approx C_{\mathrm{Butler}} = \begin{cases} 2\pi^2 D\epsilon_0/\ln(16D/H) & H/D \lesssim 4 \\ -2\pi H\epsilon_0/[1 + \ln(D/(4H))] & H/D \gtrsim 4 \end{cases}$$
(105)

$$C_0 \approx C_{\mathrm{Smythe}} = \epsilon_0 D \left[4.00 + 3.475(H/D)^{0.76}\right]$$
(106)

where ϵ_0 is the vacuum permittivity. These assume no dielectric external to the coil, but the effects of the coil form and wire insulation should be reasonably small (the field is shielded in the interior and between turns for C_0, though not for the inter-turn couplings). They also assume no perturbing conductors are nearby. The Butler result is for hollow tubes and should be widely applicable (Ref. 27 examined it for $1/4 < H/D < 200$ and found a worst error of about 4%). The Smythe case is for a solid right cylinder with conductive endcaps and meant only for $1/8 < H/D < 8$.

The sheath helix model[24,25] provides an estimate of

$$c(k) = \frac{2\pi\epsilon_0}{I_0(kD/2)K_0(kD/2)}.$$
(107)

for a free coil (no dielectric) with $H = \infty$. (If I haven't goofed the transcription: There's a factor of 2 disagreement between my references.) Numerically, $c(k)$ sharply increases from 0

before leveling, and then increases monotonically as k grows. Using Mathematica, expanding in k readily gives a series in even powers of kD,

$$c(k) \approx 2\pi\epsilon_0 \left\{ \frac{1}{\ln(kD) - 0.8091} + 0.1250 \left(\frac{\ln(kD) - 1.309}{[\ln(kD) - 0.8091]^2} \right) (kD)^2 \right.$$
$$\left. + 0.009766 \left(\frac{\ln(kD)^2 - 2.668\ln(kD) + 1.904}{[\ln(kD) - 0.8091]^3} \right) (kD)^4 + \dots \right\}, \quad (108)$$

and each coefficient for the k^{2p} term provides an estimate of $\bar{\mathcal{S}}_{\mathrm{tt}}^{(2p)}$.

There is another way to estimate the first elastance $\bar{\mathcal{S}}_{\mathrm{tt}}^{(2)}$. In the long-wavelength approximation, (41) provides the effective capacitance for a solenoid with a linear voltage gradient and grounded at one end. The first term involves $c(x)$, which assumes there is no energy stored by electric fields inside the coil interior. However, when there is a linear voltage profile, the electric field in the interior of the solenoid is expected to strongly resemble an ideal parallel plate capacitor, at least for $H \gg D$. Therefore, the energy stored by such internal fields provide a lower bound for the term involving the elastance. (Energy stored by a similar gradient outside the solenoid is ignored.) This gives the estimate

$$\frac{1}{\bar{\mathcal{S}}_{\mathrm{tt}}^{(2)}} \approx \frac{\epsilon_0 \pi D^2}{2}, \quad (109)$$

which is twice the value of the related "series capacitance parameter" C_s' from Eq. (18) of Ref. 8 because of a slightly different definition of these two parameters. Refs. 6–8 report a typical value of about $C_s' \approx 0.2$ pF m from theory and experiment. For the solenoid described in Ref. 16, (109) gives a rough estimate of $1/\bar{\mathcal{S}}_{\mathrm{tt}}^{(2)} \approx 0.4$ pF m. Ref. 28 provides theory and measurement of nearest-neighbor turn capacitances $C_{(1)}$, so could be used as an alternate approach to estimate $\bar{\mathcal{S}}_{\mathrm{tt}}^{(2)} \approx \bar{\mathcal{S}}_{\mathrm{tt,1}}^{(2)}$.

D.   Phase velocity and relationship between inductances and capacitances

In a classic uniform transmission line, the distributed inductance l and capacitance c are constrained to give the speed of light

$$v_c = 1/\sqrt{\mu_0 \epsilon_0} \quad (110)$$

as their phase velocity: $v_p = \omega(k)/k = 1/\sqrt{lc} = v_c$. This follows from connecting formulas for the scalar and vector potentials by relating the local current density with the local charge times a velocity vector along the wire direction.

In a solenoid, even with all the longitudinal couplings, it's empirically known that the axial phase velocity is approximately the speed of light along the winding direction,

$$v_p \approx v_c \sin(\psi), \quad (111)$$

up to order unity, making solenoids "slow-wave" structures (e.g., p. 476 of Ref. 23). Relatedly, the resonances of an unloaded solenoid empirically tend to occur when the winding
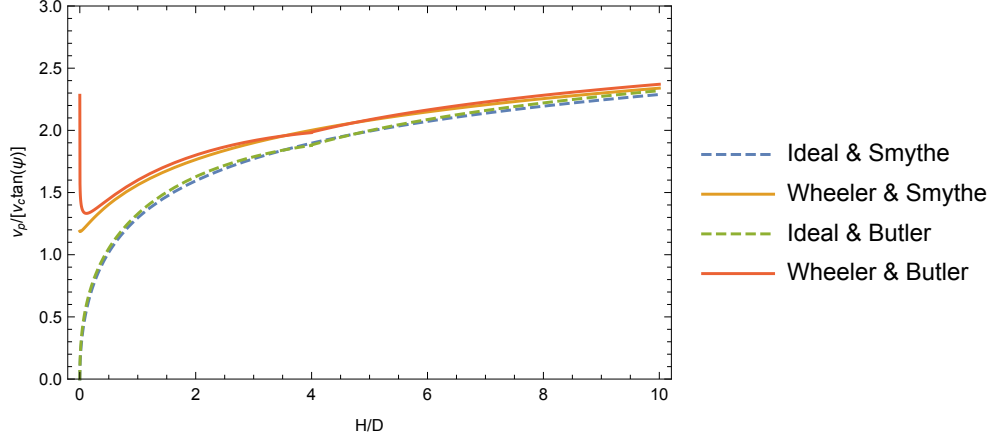
FIG. 2.   Phase velocity for a solenoid estimated using (113) with (96), the uniform inductances (97) or (98), and the uniform capacitances (105) or (106).

length is comparable to (but not exactly[b]) a number of quarter or half wavelengths in free space. In the sheath-helix model[24,25] the axial phase velocity is

$$v_p = v_c \tan(\psi) \sqrt{\frac{I_0(kD/2)K_0(kD/2)}{I_1(kD/2)K_1(kD/2)}}. \tag{112}$$

Numerically, $\tan(\psi) \approx \sin(\psi)$ for large N (small ψ), and this velocity is nearly v_c for $kD \gtrsim 3$ but grows above this to diverge as $kD \longrightarrow 0$.

   This suggests that $c(x)$ and $l(x)$ [or $c(k)$ and $l(k)$] are similarly related for a real solenoid: $l(x)c(x) \approx 1/v_c^2$ (maybe?). Perhaps this could be used to estimate the more difficult to calculate $c(x)$ from the easier $l(x)$? This would only be true for certain circumstances without environmental perturbation. For example, the shapes of $l(x)$ and $c(x)$ near the ends are complementary in a way that roughly preserves their product $l(x)c(x)$, but shielding from nearby conductors tends to smooth $c(x)$ but not $l(x)$ near the edges. Perhaps there is a way to think through how all the M_{nj} and C_{nj} coefficients, absent environmental perturbations, may be related to show this? This note's already too long as is, so, maybe for the future . . .

   As a final teaser, note that we can estimate the phase velocity with the following trick

$$\frac{v_p}{v_c \sin(\psi)} \approx \frac{v_p}{v_c \tan(\psi)} \approx \frac{1}{\sqrt{(l/\mu_0)(c/\epsilon_0)} \, \tan(\psi)} \approx \frac{\pi}{\sqrt{\left(\frac{L_0}{\mu_0 D N^2}\right)\left(\frac{C_0}{\epsilon_0 D}\right)}} \tag{113}$$

using the uniform capacitance C_0 and inductance L_0. If you use the Butler or Smythe formulas for C_0 and the ideal or Wheeler formulas for L_0, the effective phase velocity is very nearly the speed of light along the winding as shown in Fig. 2. Note that L_∞ and C_{Butler} diverge at $H/D = 0$, so the only combination that doesn't diverge is Smythe and Wheeler.

---

[b] For a numerical exploration, see "Wire length quarterwave" here: `http://abelian.org/tssp/misc.html`
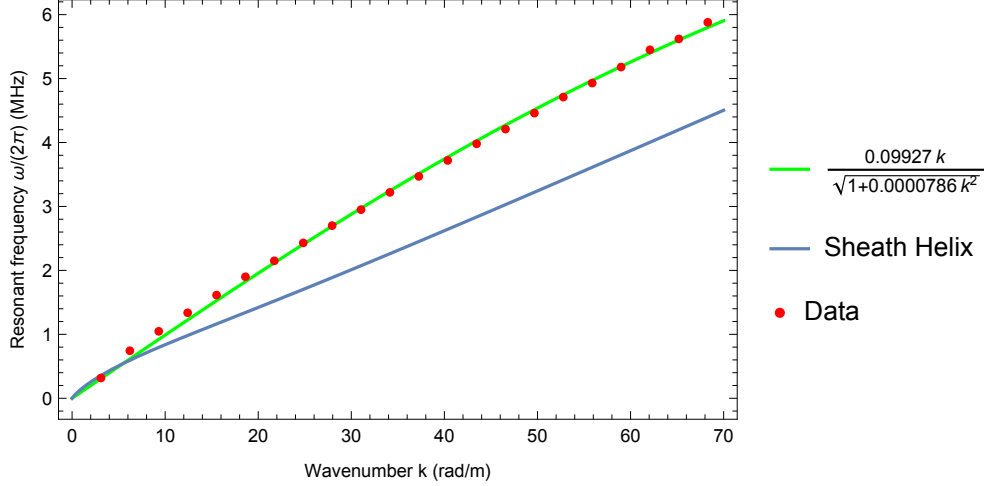
FIG. 3. Dispersion data from Ref. 16. The error bars are too small to display. Includes a sheath-helix estimate and an empirical fit curve that provides an estimate for $\bar{\mathcal{S}}_{\text{tt},1}^{(2)}$.

E. Dispersion relation, resonances, and band structure

Solenoids are wave propagating media with periodic symmetry so are known to have band structure. All of this note is restricted to the lowest so-called T_0 band with azimuthal symmetry, below any potential first cutoff before azimuthally asymmetric bands begin. The harmonic-signal approximation provided an estimate of the form of the dispersion relation $\omega(k)$. Roughly, it's shape can be probed by measuring the unloaded quarter- and half-wave resonances of a finite solenoid, which could be used to infer parameters. Neat demonstrations of such resonances worth looking up are old Seibt coils and the mood-ring-style images in Ref. 29.

Fig. 3 shows such data for the solenoid described in Ref. 16, treating the n-th resonance as having $k = \pi n/(2H)$ for $n = 1, 2, 3 \ldots$ Similar curves are shown in Refs. 6 and 7. Fig. 3 also includes the dispersion relation of the sheath helix model[24,25]

$$\omega^2 = v_c^2 \tan(\psi)^2 \, k^2 \, \frac{I_0(kD/2)K_0(kD/2)}{I_1(kD/2)K_1(kD/2)} \tag{114}$$

using (96), which ignores edge effects and assumes ϵ_0 and μ_0 everywhere. As shown, the resemblance is not terrible but also not great.

Fig. 3 also includes a rough fit of the form (93) which gives $v_p(k=0) \approx 624{,}000 \pm 6{,}000$ m/s $\approx (0.00208 \pm 0.00002)v_c$. For that solenoid, using (96) gives $\tan(\psi) \approx 0.0013$, which is reasonably close (v_p is expected to be larger than this from the sheath helix model for such small kD). Assuming that simple form, the curvature coefficient provides an estimate of $1/\left[c\,\bar{\mathcal{S}}_{\text{tt},1}^{(2)}\right] = H/\left[C_0\,\bar{\mathcal{S}}_{\text{tt},1}^{(2)}\right] \approx 0.0000786 \pm 0.0000085$ m². (There's no meaningful difference between using $\bar{\mathcal{S}}_{\text{tt}}^{(2)}$ and $\bar{\mathcal{S}}_{\text{tt},1}^{(2)}$ here.) Using an unreported measurement of $C_0 \approx 22 \pm 2$ pF for that solenoid,[16] this gives $1/\bar{\mathcal{S}}_{\text{tt},1}^{(2)} \approx 0.0034 \pm 0.0005$ pF m, which is much less than estimates discussed above. This disagreement likely comes from comparing a simplistic model fit with crude energy estimates from above.

Finally, it's fun to suppose that such dispersion relations could be measured for a solenoid wound out of coax. This way, you could compare the same geometry but with the inter-turn capacitances allowed or shielded, depending on how you use the inner and outer conductors of the coax.

1.   Cutoff suppression by mutual inductance

(Added April 2023) Ref. 30 provides an interesting historical discussion and critique of the common perception that inter-turn couplings introduce a cutoff frequency, such as occurs in the dispersion relation (93) for the simple model of Section V D. Importantly, Ref. 30 argues that the inductive couplings between turns generally suppress such a cutoff in transmission-line modeling of infinite, uniform lines, because any physical coupling must satisfy $\lim_{k \to \infty} l(k) = 0$. To see why, note that the lossless dispersion relation (92) of an infinite line does not have a cutoff for such an $l(k)$, assuming $c(k)$ does not intervene (i.e., $c(k)$ is finite throughout the limit). The sheath helix model provides support, because its dispersion relation (114) does not have a cutoff and its inductance (103) satisfies $l(\infty) = 0$.

REFERENCES

[1]B. McGuyer, "Paul Drude's Prediction of Nonreciprocal Mutual Inductance for Tesla Transformers," PLoS ONE 9, e115397 (2014). Available online: `https://doi.org/10.1371/journal.pone.0115397`

[2]B. H. McGuyer, "Deriving the equivalent circuit of a Tesla coil," technical note, 2020. Available online: `https://bartmcguyer.com/notes/note-11-TcEquations.pdf`

[3]B. H. McGuyer, "Test of the Miller self-capacitance of a solenoid inductor," technical note, 2021. Available online: `https://bartmcguyer.com/notes/note-12-MillerCapTest.pdf`

[4]Paul Nicholson and the Tesla Secondary Simulation Project Collaboration (2001). See "Theory Notes" (pn2511) and "More Theory Notes" (pn1401) documents. Available online: `http://abelian.org/tssp/`

[5]Kurt Nalty, "Transmission Lines, Stacked Insulated Washers Lines, Tesla Coils and the Telegrapher's Equation," (2008). Available online (archived): `https://web.archive.org/web/20180821213405/http://www.kurtnalty.com/TeslaCoil.pdf`

[6]B. A. Aničin, D. M. Davidović, P. Karanović, V. M. Miljević and V. Radojević, "Circuit properties of coils," in IEE Proceedings - Science, Measurement and Technology **144**, 234 (1997). DOI: 10.1049/ip-smt:19971316

[7]B. A. Aničin, "Circuit theory of video delay lines," IEEE Proceedings - Microwaves, Antennas and Propagation **146**, 65 (1999). DOI: 10.1049/ip-map:19990138

[8]B. A. Aničin, "Transmission line parameters of video delay lines," IEEE Proceedings - Microwaves, Antennas and Propagation **146**, 355 (1999). DOI: 10.1049/ip-map:19990666

[9]P. A. Abetti and F. J. Maginniss, "Fundamental Oscillations of Coils and Windings [includes discussion]," Transactions of the American Institute of Electrical Engineers. Part III: Power Apparatus and Systems, Volume 73, pp. 1–10 (1954). DOI: 10.1109/AIEEPAS.1954.4498782

[10]W. J. Herrera and R. A. Diaz, "The geometrical nature and some properties of the capacitance coefficients based on Laplace's equation" American Journal of Physics **76**, 55 (2008). DOI: 10.1119/1.2800355

[11]T. M. Minteer, "The many capacitance terms of two parallel discs in free space," European Journal of Physics **35**, 035022 (2014). DOI: 10.1088/0143-0807/35/3/035022

[12]J. M. Miller, "Electrical oscillations in antennas and inductance coils," Proc. IRE 7, pp. 299–326 (1919). DOI: 10.1109/JRPROC.1919.217442

[13]B. H. McGuyer, "Deriving the equivalent circuit of a Tesla magnifier," technical note, 2024.
Available online: `https://bartmcguyer.com/notes/note-17-MagnifierEquations.pdf`

[14]Wikipedia, "Finite Difference," accessed 2021.
Online: `https://en.wikipedia.org/wiki/Finite_difference`

[15]Wikipedia, "Fourier Transform," accessed 2021. See the non-unitary, angular frequency column in the Tables of Important Fourier Transforms. Online: `https://en.wikipedia.org/wiki/Fourier_transform`

[16]Bart McGuyer, "(Dataset) Measured self-resonant frequencies of an air-cored single-layer solenoid inductor," Harvard Dataverse, V1 (2020). `https://doi.org/10.7910/DVN/QV8HQS`

[17]T. H. Lee, *Planar Microwave Engineering*, Cambridge (2004). See Ch. 6.5.2.

[18]D. W. Knight, "Solenoid impedance and Q," (2016).
Online: `http://www.g3ynh.info/zdocs/magnetics/solenz.html`

[19]F. W. Grover, "Methods for the derivation and expansion of formulas for the mutual inductance of coaxial circles and for the inductance of single-layer solenoids," Bur. Stand. J. Res. Vol. 1, No. 4, p. 487 (1928).
Available online: `https://nvlpubs.nist.gov/nistpubs/jres/1/jresv1n4p487_A1b.pdf`

[20]E. B. Rosa and F. W. Grover, "Formulas and tables for the calculation of mutual and self inductance," Bur. Stand. J. Res. Vol. 8, No. 1, p. 1 (1916).
Available online: `https://archive.org/details/formulastablesfo813rosa`

[21]D. W. Knight, "An introduction to the art of solenoid inductance calculation," (2016).
Online: `http://www.g3ynh.info/zdocs/magnetics/part_1.html`

[22]R. Lundin, "A Handbook Formula for the Inductance of a Single-Layer Circular Coil," Proceedings of the IEEE **73**, 1428, (1985). DOI: 10.1109/PROC.1985.13304

[23]S. Ramo, J. R. Whinnery, and T. Van Duzer, *Fields and Waves in Communication Electronics*, Wiley (1994), 3rd ed.

[24]J. E. Rowe, *Nonlinear Electron-Wave Interaction Phenomena,* Academic Press (1965). See Chapter 3.3.

[25]F. S. Chute and F. E. Vermeulen, "On the self-capacitance of solenoidal coils," Canadian Electrical Engineering Journal **7**, 31–37 (1982). DOI: 10.1109/CEEJ.1982.6594621

[26]J. D. Jackson, "Charge density on a thin straight wire: The first visit," American Journal of Physics **70**, 409 (2002). DOI: 10.1119/1.1432973

[27]C. M. Butler, "Capacitance of a finite-length conducting cylindrical tube," J. Appl. Phys **51**, 5607 (1980). DOI: 10.1063/1.327575

[28]G. Grandi, M. K. Kazimierczuk, A. Massarini, and U. Reggiani, "Stray Capacitances of Single-Layer Solenoid Air-Core Inductors," IEEE Transactions on Industrial Applications **35**, "62 (1999). DOI: 10.1109/28.793378

[29]F. S. Chute and F. E. Vermeulen, "A Visual Demonstration of the Electric Field of a Coil Carrying a Time-Varying Current," IEEE Transactions on Education, Volume E-24, pp. 278–283 (1981). DOI: 10.1109/TE.1981.4321510

[30]D. Bormann, "Exactly solvable high frequency model of a coil of finite length," Progress in Electromagnetics Research Symposium (PIERS 2013 Stockholm) Proceedings, Volume 1, pp. 951-955 (2013). Available online: `https://www.researchgate.net/publication/286610068_Exactly_solvable_high_frequency_model_of_a_coil_of_finite_length`